One-dimensional three-body problem via symbolic dynamics

Kiyotaka Tanikawa[1] and Seppo Mikkola[1,2]
谷川清隆、セッポ ミッコラ

[1]National Astronomical Observatory, Mitaka, Tokyo 181, Japan
[2]Tuorla Observatory, University of Turku, 21500 Piikkiö, Finland

Abstract

Symbolic dynamics is applied to the one-dimensional three-body problem. The sequence of collisions along an orbit is expressed as a symbol sequence of three symbols. We find systematically sequences of collisions which are unallowable. There is an infinite number of periodic sequences which suggests an infinity of periodic orbits other than the Schubart orbit. Under reasonable assumptions on unallowable sequences, we prove that symbol sequences form a Cantor set.

Key words: one dimensional three-body problem – symbolic dynamics – chaos

1   Introduction

One-dimensional three-body systems starting from general initial conditions have been extensively studied by Mikkola and Hietarinta(1989; 1990; 1991). Tanikawa & Mikkola(1999; hereafter referred to as Paper I) introduced symbol sequences and found that triple-collision orbits can be obtained easily as boundaries of different symbol sequences. (For the application of symbol sequences to the three-body problem, see also Zare & Chesley, 1998). They found that the region of the phase space so far considered chaotic is stratified by regions separated by triple-collision curves, i.e., curves formed by initial conditions leading to triple collision.

The present paper is the extension of Paper I. Our purpose here is to understand more deeply the structure of the phase space of the one-dimensional three-body problem and to get an insight into its dynamics. Instead of considering orbits themselves, we consider the set of symbol sequences constructed from the sequences of binary collisions along orbits. Our main results are as follows. We divide the surface of section into five regions with different types of symbol

sequence and use the symmetry of the surface of section. Then we find that there are unallowable sequences of collisions. Next, we find that the surface of section is rather simply stratified by bands of points with symbol sequences with increasing or decreasing order when considered as decimal numbers. Based on this fact, the existence of periodic orbits and other orbits are shown. Finally, based on the numerical results, we prove that the set of allowable symbol sequences form a Cantor set in the set of all symbol sequences.

2 Formulation of the Problem

We put three mass points m_1, m_0, and $m_2 (m_0 = m_1 = m_2)$ in this order on a line. Fix the masses and the gravitational constant to one. Then the Hamiltonian of the problem is given (1, Mikkola & Hietarinta, 1989) by

$$H = \frac{1}{2} \sum_{i=0}^{2} w_i^2 - \sum_{i<j} \frac{1}{|x_i - x_j|}. \tag{2.1}$$

where w_i are momenta conjugate to the coordinates x_i on the line. We have $x_1 \le x_0 \le x_2$. Introducing new coordinates by

$$\begin{aligned} q_1 &= x_0 - x_1, \\ q_2 &= x_2 - x_0, \end{aligned} \tag{2.2}$$

we get the new Hamiltonian as

$$H = p_1^2 + p_2^2 - p_1 p_2 - \frac{1}{q_1} - \frac{1}{q_2} - \frac{1}{q_1 + q_2}. \tag{2.3}$$

We fix the total energy to -1 and start the integration at $q_1(0) = q_2(0) = R$. This means that two outer particles are placed in an equal distance from the central. Then the value of potential is fixed to $2.5/R$. The kinetic energy T is determined by

$$T = 2.5/R - 1. \tag{2.4}$$

Initial zero velocities correspond to $R = 1/2.5$.

If we introduce a parametrization

$$\begin{aligned} \sqrt{3}(p_1 - p_2) &= 2\sqrt{T} \sin\theta, \\ (p_1 + p_2) &= 2\sqrt{T} \cos\theta, \end{aligned} \tag{2.5}$$

then (θ, R) specify the initial value. Velocities are given by R and θ as

$$\begin{aligned} \dot{q}_1 &= 2p_1 - p_2 = 2\sqrt{T} \cos(\theta - \pi/3) \\ \dot{q}_2 &= 2p_2 - p_1 = 2\sqrt{T} \cos(\theta + \pi/3). \end{aligned} \tag{2.6}$$

The function $S = p_1 Q_1^2 + p_2 Q_2^2$ generates the additional transformation with the new coordinates $Q_1 = \sqrt{q_1}$, $Q_2 = \sqrt{q_2}$ and new momenta $P_i = 2 Q_i p_i$. If accompanied with the time transformation $t' = q_1 q_2$ the regularized new Hamiltonian

$$\Gamma = \frac{1}{4}(P_1^2 Q_2^2 + P_2^2 Q_1^2 - P_1 P_2 Q_1 Q_2) - Q_1^2 - Q_2^2 - Q_1^2 Q_2^2/(Q_1^2 + Q_2^2) - Q_1^2 Q_2^2 E, \quad (1)$$

is obtained. Here E is the (initial) numerical value of the Hamiltonian. The equations of motion following from this Hamiltonian can be integrated numerically with conventional methods, such as the Bulirsch-Stoer integrator (Bulirsch & Stoer 1966).

We start integration from the state $q_1 = q_2$ with $0 \leq \theta < \pi$. For our fixed energy, initial states can be expressed in a surface of section H:

$$H = \{(\theta, R) \mid 0 \leq \theta < \pi, 0 \leq R \leq 2.5\}.$$

To obtain the global structure, we cover surface of section H with a mesh of grid size $(\Delta R, \Delta \theta) = (0.002, 0.°1)$ and integrate orbits starting at each vertices of grids forward until the 66th binary collision is obtained. The total number of orbits amounts to 2.25×10^6. To obtain particular local structure, we perform additional integrations with finer mesh.

3   Symbol Sequences and Surface of Section

There can be three types of collision along an orbit: binary collisions between m_1 and m_0 and between particles m_0 and m_2 and a triple collision. Let us denote a binary collision between m_0 and m_1 by '1' and a binary collision m_2 and m_0 by '2', and a triple collision by '0'. A symbol sequence is constructed in such a way that when m_0 and m_1 collide, the symbol '1' is added to the sequence and when m_2 and m_0 collide the symbol '2' is concatenated.

Let us express an orbit as a sequence of $0, 1$ and 2 as follows:

$$(\ldots n_{-2} n_{-1}.n_0 n_1 n_2 \ldots)$$

where $n_i, i \in \mathbf{Z}, i \neq 0$ are either $0, 1$, or 2.

We follow the orbit starting from the initial condition defined in §2 to the future and to the past. Then n_0 represents the first collision. n_1 and n_2 represent the type symbol of the second and third next binary collisions, and so on. Similarly, $n_{-1}, n_{-2}, \ldots$ represent the type symbol of the past collisions.

Let Σ denote the set of all bi-infinite sequences $s = (\ldots n_{-2} n_{-1}.n_0 n_1 n_2 \ldots)$. We define a metric on Σ setting $\mathrm{d}(s, s) = 0$ and $\mathrm{d}(s^1, s^2) = 3^{-|m|}$ if $s^1 \neq s^2$ and

$|m|$ is the least integer such that $s_m^1 \neq s_m^2$(Block & Coppel, 1992). Then Σ is a compact metric space. Let us define

$$\Sigma_2 = \{s \in \Sigma \mid s_i = 1 \text{ or } 2\}.$$

Then it is known that Σ_2 is a Cantor set(Robinson, 1995). In other words, symbol sequences corresponding to orbits which repeat binary collisions form a Cantor set in the whole sequence space Σ.

The shift operator σ is defined by

$$\sigma(\ldots n_{-2}n_{-1}.n_0 n_1 n_2 \ldots) = (\ldots n_{-2}n_{-1}n_0.n_1 n_2 \ldots)$$

on Σ.

Remark. We cannot directly obtain orbits which start and/or end at triple collision. In our numerical study, though we assigned symbol '0' to triple collision, we actually work in the space Σ_2. Symbol sequences containing '0' can be obtained only as a boundary of symbol sequences not containing '0'. This has been the main result of paper I.

The correspondence between a symbol in a sequence and a point in the surface of section is not one-to-one. It follows from the following propositions that if the orbit appears again on the surface H, then the preceding and succeeding binary collisions occur with m_1 and m_0 and with m_2 and m_0, respectively. To put it differently, the period(present) can only be inserted between successive '1' and '2' in this order. An orbit does not appear on H as long as binary collisions between the same particles are repeated.

Proposition 3.1. A trajectory in the (q_1, q_2)-plane crosses transversely the homographic line except at $(\theta, R) = (0, 0)$, if it does at all.

Proof. If $q_1 = q_2$ and $\dot{q}_1 = \dot{q}_2$, the solution is homographic and always on the homographic line. So the trajectory initially outside the homographic line never become tangent to the line except the case of triple collision. $\square$

Proposition 3.2. If a trajectory crosses the homographic line on the (q_1, q_2)-plane, a binary collision occurs before the trajectory again crosses it.

Proof. Suppose that a trajectory crosses the homographic line from $(q_1 < q_2)$-side to $(q_1 > q_2)$-side at $t = t_0$, i.e., $q_1 = q_2$ and $\dot{q}_1 > \dot{q}_2$ at $t = t_0$. Then there exists a small $\varepsilon > 0$ such that $q_1 > q_2$ and $\dot{q}_1 > \dot{q}_2$ at $t = t_0 + \varepsilon$. This implies that there needs a finite time in order to again cross the homographic line. Suppose that the first crossing occurs at $t = t^* > t_0$ without binary collision during (t_0, t^*). We can use the continuity argument in this case. At $t = t^*$, we should have $q_1 = q_2$ and $\dot{q}_1 < \dot{q}_2$ by Proposition 3.1. In order to have this, we should have $q_1 > q_2$
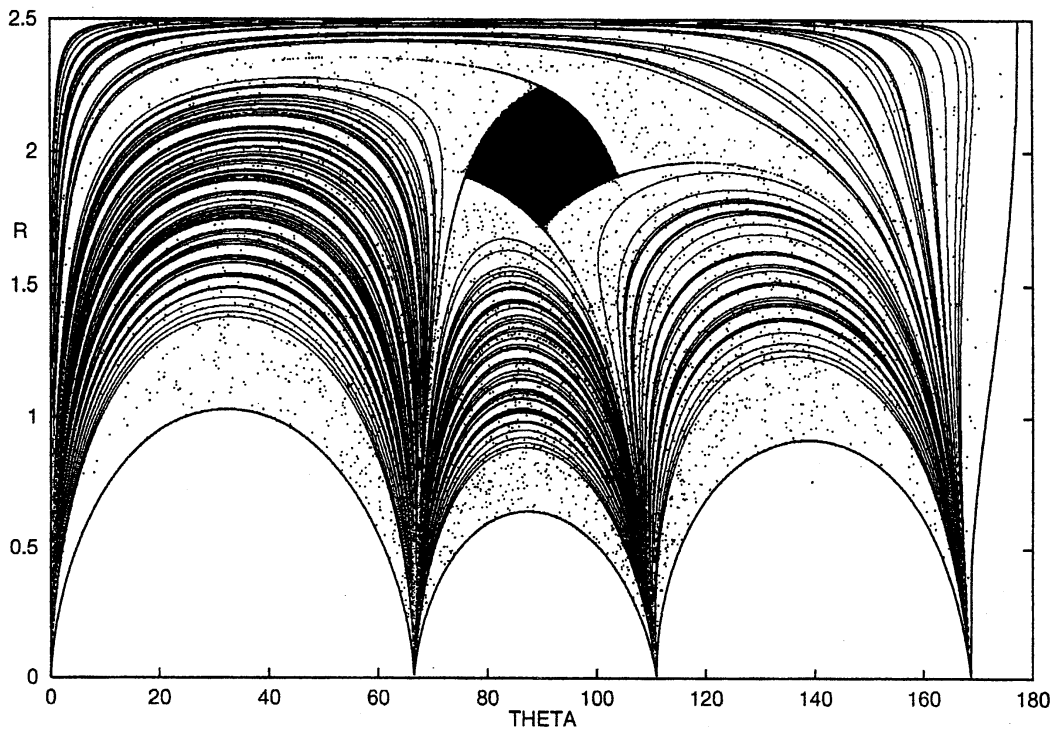
Figure 1: Stratified structure of the surface of section. Reproduction of Fig.5 in Paper I. Shown are the Schubart region(black), triple collision curves, and immediate escape reions(blank).

and $\dot{q}_1 = \dot{q}_2$ at some $t^{**}, t_0 < t^{**} < t^*$. We should have in turn $\ddot{q}_2 > \ddot{q}_1$ at least at some time between t_0 and t^{**}. This implies $q_2 < q_1$ at the same instant, which is a contradiciton. □

Finally, the surface of section has a symmetry due to the reversibility of the problem. The past orbit starting at point (θ, R) is realized by the future orbit starting at point $(\pi - \theta, R)$ with particle names m_1 and m_2 exchanged. Thus, to obtain the orbits for $-\infty < t < \infty$ of all the points of the surface of section, we need only to integrate their orbits for $0 \leq t < \infty$.

4 Orbits and Symbol sequences

4.1 Global structure of the Surface of Section

In paper I, we observed that the surface of section H is divided into smaller parts by points with different symbol sequences. In fact, H is divided into two regions of points having symbol sequence $1.22\ldots$ and $1.21\ldots$ It is divided into four by symbol sequence $1.222\ldots$, $1.221\ldots$, $1.211\ldots$, and $1.212\ldots$ It is divided

into seven by sequences 1.2222..., 1.2221..., 1.2212..., 1.2122..., 1.2121..., 1.2112..., and 1.2111..... An so on. The boundary of regions of different symbol sequences form curves and this curve turned out to be initial conditions of triple collision. We called these curves *triple collision curves*. Thus the surface of section is divided into increasing number of smaller parts with increasing number of digits of symbol sequences. (see Fig.1, a reproduction of Fig.5 in paper I.)

In paper I, we did not consider the organization or distribution of various regions with respect to different symbol sequences. In the present paper, our target is to know the detailed structure of the surface of section and get an insight into the dynamics of the one-dimensional three-body problem. The first important observation is that there is a large structure in H. Four curves seem to emanate from the corner of the black region, i.e. the 'Schubart region' surrounding the stable periodic orbit called the Schubart orbit, and reach the bottom boundary of the surface of section. In Fig. 1, these four curves are obtained as a subset of scattered orbits starting just outside the Schubart region.

In order to confirm that these are actually curves, we performed orbit intergrations with initial conditions along short segments across these supposed curves. The grid size is as small as $0°.001$ for horizontal search, and it is 0.0001 for vertical search. A point is considered to be on the curves if the corresponding symbol sequence is of the form $1.(21)^n$ with $n \geq 36$. Near the boundary of the Schubart region, more digits are required. Moreover, there we interpolated the position of the curve when more than one grid points satisfy the condition.

The result is shown in Fig.2(a). Four curves seem smoothly connected to the boundary of the Schubart region. We denote the regions separated by these curves by S, $\mathcal{L}$, $\mathcal{C}$, $\mathcal{R}$, and $\mathcal{T}$, meaning the Schubart region, left, center, right, and top regions, respectively. The corresponding symbol sequences are given in Table I. Here, for example, $(21)^n$ means $2121\ldots21(n$ times).

Table I. Symbol sequences in the surface of section.

Region	Sequence($n \geq 0$)
S	$(21)^\infty.(21)^\infty$
$\mathcal{L}$	$\ldots1.(21)^{2n}22\cdots$
$\mathcal{C}$	$\ldots1.(21)^{2n+1}1\cdots$
$\mathcal{R}$	$\ldots1.(21)^{2n+1}22\cdots$
$\mathcal{T}$	$\ldots1.(21)^{2n+2}1\cdots$

Remark. The division into S, $\mathcal{L}$, $\mathcal{C}$, $\mathcal{R}$, and $\mathcal{T}$ is based on the numerical result that triple collision curves do not cross the boundaries of these regions. One should be careful that the division seen in Fig.2(a) may not be exact near the boundary of S. There is a pair of period-2 points around the Schubart region.
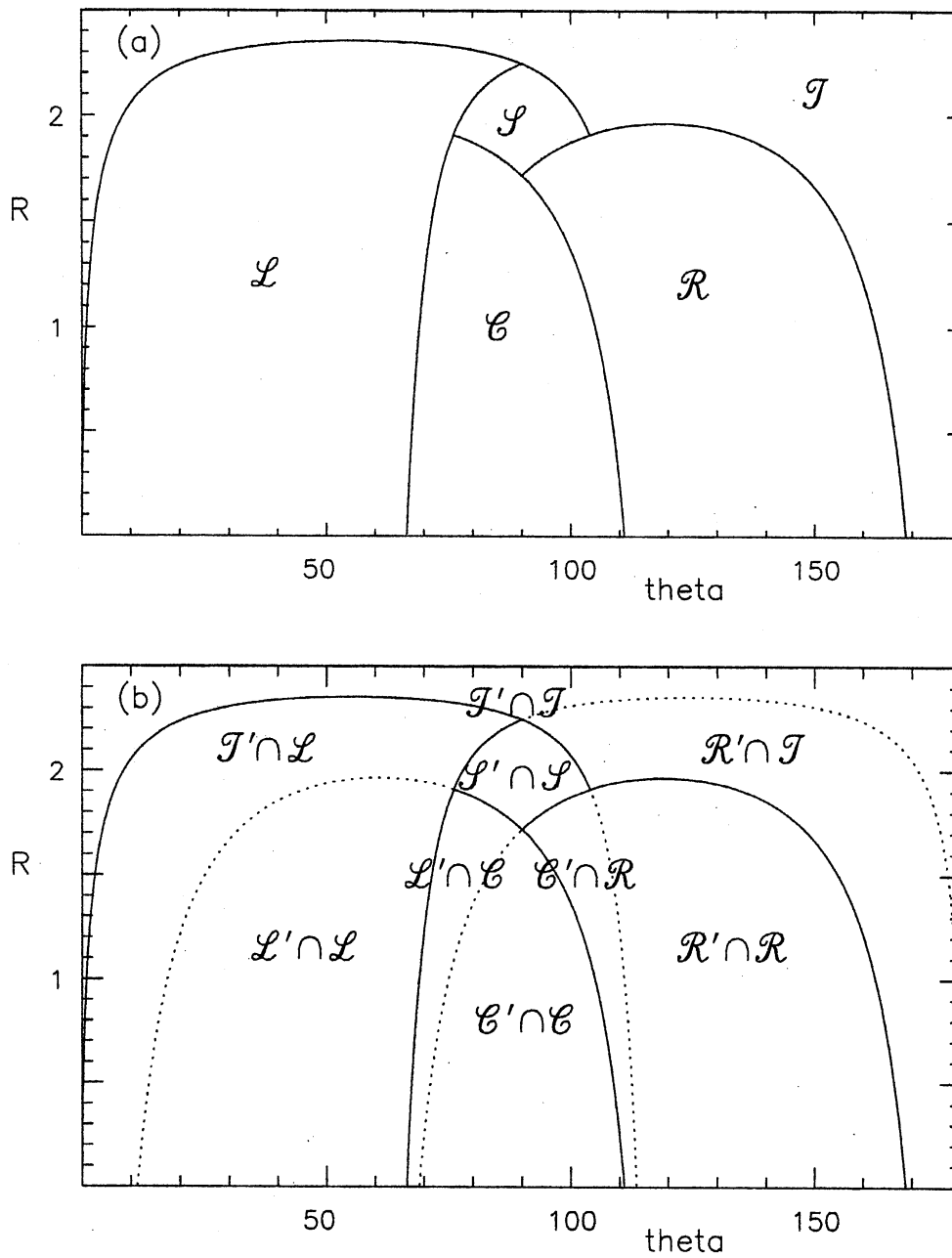
Figure 2: (a) Division of the surface of section. (b) Overlapping regions of the surface of section and its reverse.

These points at the corners of the Schubart region and the outermost KAM curve of the Schubart region are expected disjoint. Near the boundary of the Schubart region, $\mathcal{L}$, $\mathcal{C}$, $\mathcal{R}$, and $\mathcal{T}$ may be intermingled in a complicated manner. In this paper, we will not draw any conclusion related to this area.

4.2   Unallowable symbol sequences

As we pointed out in §3, the surface of section has a symmetry. The past history of the orbit starting at (θ, R) is realized by the future of the orbit starting at $(\pi - \theta, R)$ and vice versa. Thus, in order to get the bi-infinite symbol sequence of an orbit starting at (θ, R), (i) we calculate the future orbit starting at (θ, R) and record its future symbol sequence $1.2c_2c_3\ldots$, (ii) calculate the future orbit starting at $(\pi - \theta, R)$ and record its future symbol sequence $1.2s_2s_3\ldots$, (iii) make a *past* symbol sequence $\ldots \bar{s}_3\bar{s}_21.2$ where $\bar{s} = 1$ or 2 according as $s = 2$ or 1, and (iv) concatenate two symbol sequences as $\ldots \bar{s}_3\bar{s}_21.2c_2c_3\ldots$.

The above procedure suggests us to check whether or not a given symbol sequence is *allowable*(i.e., realizable as a sequence of collisions). If an arbirary future symbol sequence can be concatenated with an arbitray past symbol sequence, then any bi-infinite symbol sequence is allowable.

Let us reverse the surface of section H with transformation $\theta \rightarrow \pi - \theta$ and call the resultant surface H^t the reversed surface of section. Let us denote respectively by $\mathcal{L}', \mathcal{C}', \mathcal{R}'$ and $\mathcal{T}'$ the regions of H^t. Here for example, $\mathcal{L}'$ is the original $\mathcal{R}$ if not reversed. The corresponding sequences (for the past) with '1' and '2' exchanged are given in Table II.

Table II. Symbol sequences in the reversed surface of section.

Region	symbol sequence($n \geq 0$)
$\mathcal{L}'$	$\ldots 11(21)^{2n+1}.2\cdots$
$\mathcal{C}'$	$\ldots 2(21)^{2n+1}.2\cdots$
$\mathcal{R}'$	$\ldots 11(21)^{2n}.2\cdots$
$\mathcal{T}'$	$\ldots 2(21)^{2n+2}.2\cdots$

If regions without prime and with prime overlap, then the symbol sequence obtained by concatenating two one-sided sequence is allowable. Otherwise the sequence is unallowable. There are 17 combinations of possible overlapping regions: 16 combinations between one of $\mathcal{L}, \mathcal{C}, \mathcal{R}, \mathcal{T}$ and one of $\mathcal{L}', \mathcal{C}', \mathcal{R}', \mathcal{T}'$ and one combination of $\mathcal{S}$ and $\mathcal{S}'$. Due to the symmetry of the problem, we have $\mathcal{S} = \mathcal{S}'$. We show the non-empty overlapping regions in Fig.2(b). As we pointed out in Remark in §4.1, near the boundary of $\mathcal{S} \cap \mathcal{S}'$ other overlappng regions may have complicated form. However, we neglect it.

Non-overlapping combinations of regions are listed in Table III together with unallowable *words*, where a word means a finite sequence of symbols. Any symbol sequence having an unallowable word as its subsequence is unallowable. This can be easily shown by using the shift operator σ.

Table III. Pairs of non-overlapping regions and unallowable words.

H^t	H	Form of symbol sequence	Unallowable word
$\mathcal{C}'$	$\mathcal{L}$	$\ldots 2(21)^{2m+1}.(21)^{2n}22\ldots$	$2(21)^{2k+1}22$
$\mathcal{R}'$	$\mathcal{L}$	$\ldots 11(21)^{2m}.(21)^{2n}22\ldots$	$11(21)^{2k}22$
$\mathcal{R}'$	$\mathcal{C}$	$\ldots 11(21)^{2m}.(21)^{2n+1}1\ldots$	$11(21)^{2k+1}1$
$\mathcal{T}'$	$\mathcal{C}$	$\ldots 2(21)^{2m+2}.(21)^{2n+1}1\ldots$	$2(21)^{2k+3}1$
$\mathcal{L}'$	$\mathcal{R}$	$\ldots 11(21)^{2m+1}.(21)^{2n+1}22\ldots$	$11(21)^{2k+2}22$
$\mathcal{T}'$	$\mathcal{R}$	$\ldots 2(21)^{2m+2}.(21)^{2n+1}22\ldots$	$2(21)^{2k+3}22$
$\mathcal{L}'$	$\mathcal{T}$	$\ldots 11(21)^{2m+1}.(21)^{2n+2}1\ldots$	$11(21)^{2k+3}1$
$\mathcal{C}'$	$\mathcal{T}$	$\ldots 2(21)^{2m+1}.(21)^{2n+2}1\ldots$	$2(21)^{2k+3}1$

There are no other unallowable words. In fact, the regions $\mathcal{L}$, $\mathcal{C}$, $\mathcal{R}$, and $\mathcal{T}$ are stratified by triple collision curves running almost parallel to their boundary inside the surface. In addition, all these stratified regions in $\mathcal{L}$, $\mathcal{C}$, $\mathcal{R}$, and $\mathcal{T}$ converge to triple collision points at the bottom of the surface of section. On the other hand, triple collision curves of the original and reversed surface of sections intersect transversely. This can be confirmed comparing Figs. 1 and 3. Therefore, if one of $\mathcal{L}$, $\mathcal{C}$, $\mathcal{R}$, and $\mathcal{T}$ has common area with one of $\mathcal{L}'$, $\mathcal{C}'$, $\mathcal{R}'$, and $\mathcal{T}'$, then the region for any sequence $(\ldots s_{-2}s_{-1}.)$ in the former and the region for any sequence $(.t_0 t_1 \ldots)$ in the latter has common points, and the concatenated sequence $(\ldots s_{-2}s_{-1}.t_0 t_1 \ldots)$ is allowable.

Proposition 4.1. Unallowable words have the form $2(21)^{2k+1}22$, $11(21)^{2k}22$, $11(21)^{2k+1}1$, and $2(21)^{2k+3}1$ for $0 \leq k \leq k_0$. Here k_0 is some large positive integer. Their lengths are $4k$ and $4k + 1$ with $k \geq 1$.

We give first several examples in Table IV. The absense of These sequences are confirmed numerically.

Table IV. Unallowable words of length less than or equl to 13.

4	5	8	9	12	13
2211	22122	22121211	221212122	221212121211	2212121212122
1122	11211	11212122	112121211	112121212122	1121212121211

Remark. In view of Remark in 4.1, we added the restriction $k \leq k_0$ in Proposition 4.1.

4.3 A detailed structure of the surface of section

In order to see the detailed distribution of symbol sequences in the surface of section, we integrated orbits along the lines $\theta = 30°$, $90°$, and $150°$ with a finer

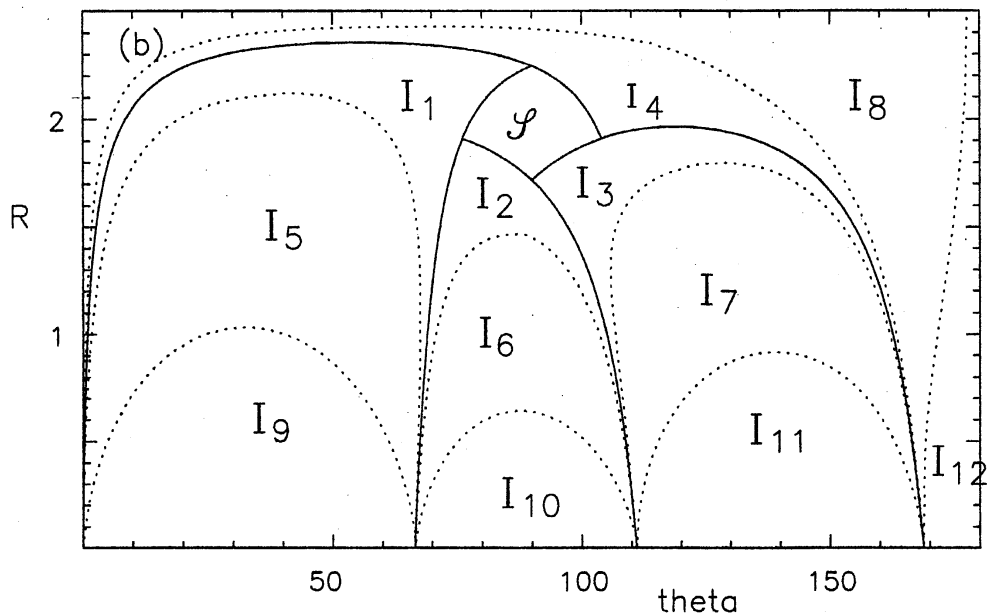Figure 3: A finer structure of the surface of section.

mesh. We find that along the line $\theta = 30°$ which is transeverse to the structure in $\mathcal{L}$, symbol sequences are distributed in such a way that symbol sequences considered as ternary or decimal numbers decrease with increase of R starting from $1.(2)^\infty$ down to $1.(21)^\infty$. We divide symbol sequences into three groups: $1.(2)^\infty$, $1.(2)^n 1 \ldots$, and $1.(21)^{2k}22\ldots$ with $n \geq 2, k > 0$. We call the regions with these symbol sequences $I_9, I_5,$ and I_1, respectively. The lack of odd exponents in the symbol sequences in I_1 will be understood if one sees the symbol sequences in I_3 introduced below.

Along the line $\theta = 90°$ and in $\mathcal{C}$, symbol sequences are distributed in such a way that symbol sequences considered as ternary or decimal numbers increase with increase of R starting from $1.2(1)^\infty$ up to $1.(21)^\infty$. We divide symbol sequences into three groups: $1.2(1)^\infty$, $1.2(1)^n 2\ldots$, and $1.(21)^{2k+1}1\ldots$ with $n \geq 2, k > 0$. We call the regions with these symbol sequences $I_{10}, I_6,$ and I_2, respectively. Similar to the case of I_1, the lack of even exponents in the symbol sequences in I_3 will be understood if one sees the symbol sequences in I_4 introduced below.

Along the line $\theta = 150°$ and in $\mathcal{R}$, symbol sequences decrease with increase of R from $1.21(2)^\infty$ down to $1.(21)^\infty$. We divide symbol sequence into three groups: $1.21(2)^\infty$, $1.21(2)^n 1\ldots$, and $1.(21)^{2k+1}22\ldots$ with $n \geq 2, k > 0$. We call the regions with these symbol sequences $I_{11}, I_7,$ and I_3, respectively.

Finally, along either of the lines $\theta = 30°, 90°$, or $150°$ and in $\mathcal{T}$, symbol

sequences increase with decrease of R from $1.212(1)^\infty$ up to $1.(21)^\infty$. We divide symbol sequence into three groups: $1.212(1)^\infty$, $1.212(1)^n 2 \ldots$, and $1.(21)^{2k}1 \ldots$ with $n \geq 2, k > 0$. We call the regions with these symbol sequences I_{12}, I_8, and I_4, respectively.

Thus there are in total twelve regions $I_i, i = 1, 2, \ldots, 12$ other than $\mathcal{S}$(see Fig.3). The boundary of I_1 and I_5 is the triple collision curve with symbol sequence $(\ldots 1.20)$. Similarly, the boundaries of I_2 and I_6, of I_3 and I_7, and of I_4 and I_8 are triple collision curves with symbol sequences $(\ldots 1.210)$, $(\ldots 1.2120)$, and $(\ldots 1.21210)$, respectively. Regions I_9, I_{10}, I_{11}, and I_{12} will be called immediate escape regions(called regular regions in Paper I) with symbol sequences $(\ldots 1.(2)^\infty)$, $(\ldots 1.2(1)^\infty)$, $(\ldots 1.21(2)^\infty)$, and $(\ldots 1.212(1)^\infty)$, respectively.

Table V. Subregions and symbol sequences

Name	Sequence $n \geq 2, k > 0, m > 0$	next	Name	Sequence $n \geq 2, k > 0, m > 0$	next
I_1	$1.(21)^{2k}22\cdots$	I_3orI_7	I_2	$1.(21)^{2k+1}1\cdots$	I_4orI_8
I_3	$1.(21)^{2k+1}22\cdots$	I_1	I_4	$1.(21)^{2k}1\cdots$	I_2
I_5	$1.(2)^n 12(1)^\infty$	I_{10}	I_6	$1.2(1)^n 121(2)^\infty$	I_{11}
	$1.(2)^n 1211\ldots$	I_6		$1.2(1)^n 121(2)^{2m}1\ldots$	I_7
	$1.(2)^n 1(21)^{2m}211\ldots$	I_2		$1.2(1)^n 1(21)^{2m}2122\ldots$	I_3
	$1.(2)^n 1(21)^{2m}2122..$	I_3		$1.2(1)^n 1(21)^{2m}21211..$	I_4
	$1.(2)^n 121(2)^{2m}1\ldots$	I_7		$1.2(1)^n 1212(1)^m 1\ldots$	I_8
	$1.(2)^n 121(2)^\infty$	I_{11}		$1.2(1)^n 1212(1)^\infty$	I_{12}
I_7	$1.21(2)^n 1\ldots$	I_5	I_8	$1.212(1)^n 2\ldots$	I_6
I_9	$1.(2)^\infty$	escape	I_{10}	$1.2(1)^\infty$	escape
I_{11}	$1.21(2)^\infty$	I_9	I_{12}	$1.212(1)^\infty$	I_{10}

We can further divide $I_i, i = 1, 2, \ldots, 8$ into smaller pieces. However, instead of doing this, we only look into a slightly finer structure of I_5 and I_6. This will be enough for finding periodic symbol sequences which will be done in §4.3.

Let us consider I_5. As we described above, symbol sequences in I_5 have the form $1.(2)^n 1 \ldots$ with $n \geq 2$ and these considered as decimal numbers decreases when R increases along the line $\theta = 30°$. So the points with symbol sequences $1.(2)^n 1 \ldots$ with larger n stays below those with smaller n. Let us fix $n \geq 2$ and look into the structure of the point set with symbol sequence $1.(2)^n 1 \ldots$. The largest symbol sequence (as a decimal number) is $1.(2)^n 1(2)^\infty$. However, this sequence is unallowable because unallowable word '22122' is contained. So the largest allowable symbol sequence is $1.(2)^n 121(2)^\infty$. Then we have $1.(2)^n 121(2)^\infty > 1.(2)^n 121(2)^m 1 \ldots > 1.(2)^n 1(21)^{2m'}22 \ldots > 1.(2)^n 1(21)^\infty > 1.(2)^n 1(21)^{2k}211 \ldots > 1.(2)^n 1211 \ldots > 1.(2)^n 12(1)^\infty$ where $m \geq 2$, $m' \geq 1$, and $k \geq 1$. In getting the above sequence of inequalities we have made use of Proposition 4.1. For example, sequence $1.(2)^n 1(21)^{2m'+1}22 \ldots$ might have been included
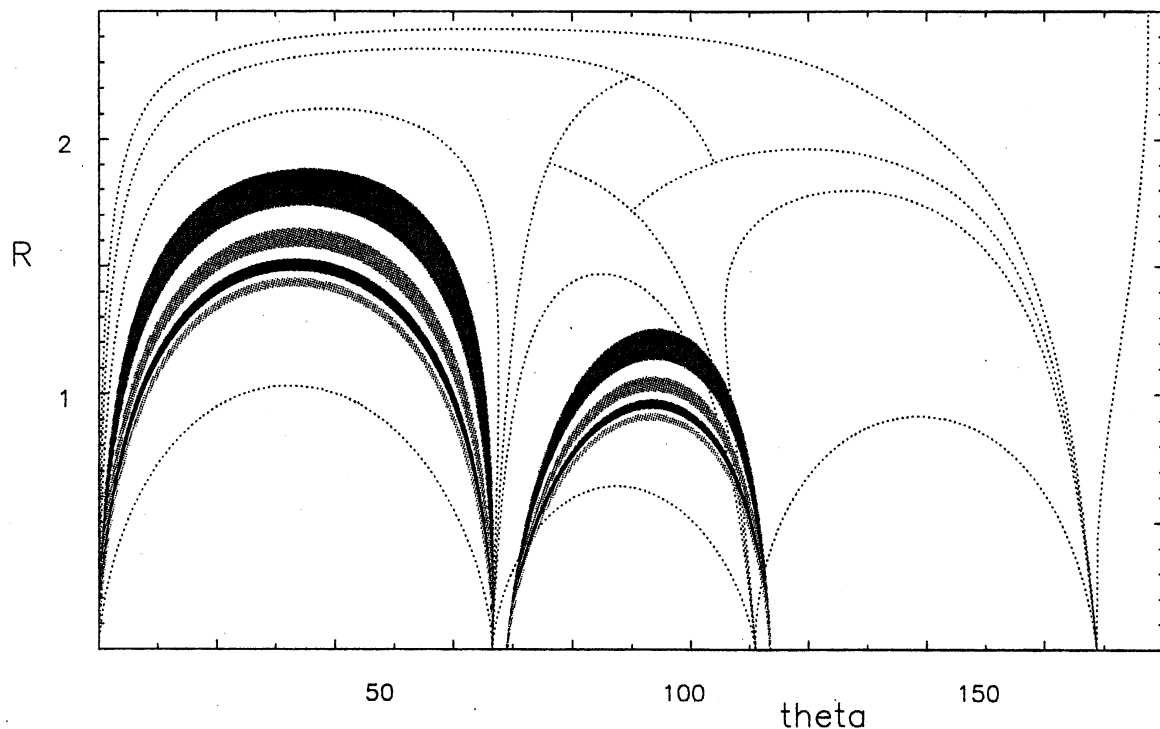
Figure 4: Mapping of regions in $\mathcal{L}$. Four bands in the left with symbol sequences $1.(2)^3 1\ldots$, $1.(2)^5 1\ldots$, $1.(2)^7 1\ldots$, and $1.(2)^9 1\ldots$, are mapped to four bands in the right. Corresponding regions have the same color.

in inequalities. However, this is unallowable because it contains unallowable word '$221(21)^{2m'+1}22$'. Now operating σ^n to these sequences, we get $1.21(2)^\infty \in I_{11}$, $1.21(2)^m 1 \ldots \in I_7$, $1.(21)^{2m'}22\ldots \in I_3$, $1.(21)^{2k}211\ldots \in I_2$, $1.211\ldots \in I_6$, and $1.2(1)^\infty \in I_{10}$. The remaining sequence $1.(21)^\infty$ is on the stable manifold which tends to one of the corner of the Schubart region. Now we conclude that orbits of points whose symbol sequences have the form $1.(2)^n 1\ldots$ cross in the next intersection the surface of section either in $I_{11}, I_7, I_3, I_2, I_6, I_{10}$ or in the boundary of $\mathcal{C}$ and $\mathcal{R}$.

Let us confirm the above consideration by numerical integration of orbits. Let us take points of region $\mathcal{L}$ whose symbol sequences are $1.(2)^3 1\ldots$, $1.(2)^5 1\ldots$, $1.(2)^7 1\ldots$, and $1.(2)^9 1\ldots$, and integrate their orbits until the next intersection with the surface of section. The results are shown in Fig. 4. We see images of the initial bands have the form also of bands and indeed pass through $I_{11}, I_7, I_3, I_2, I_6$, and I_{10}. Now it is clear that $1.(21)^\infty$, the image of $1.(2)^n 1(21)^\infty$, is on the boundary of $\mathcal{C}$ and $\mathcal{R}$.

One can do the same thing for I_6. Here we do not repeat the procedure. One sees in Table V regions $I_i, i = 1, 2, \ldots, 12$ and the corresponding symbol sequences together with the regions mapped to in the next intersection. The points in I_1

and I_3 move alternately as $I_1 \rightarrow I_3 \rightarrow I_1 \rightarrow I_3 \rightarrow \ldots$, finally make transition $I_1 \rightarrow I_7$ and go into I_5. Similarly, the points in I_2 and I_4 move alternately as $I_2 \rightarrow I_4 \rightarrow I_2 \rightarrow I_4 \rightarrow \ldots$, finally make transition $I_2 \rightarrow I_8$ and go into I_6. The initial behavior resembles that of period 2 points near the boundary of the Schubart region. The motion is almost regular revolving around the Schubart region and gradually approaching the boundary of 'chaotic regions' I_5 or I_6.

I_7 and I_8 are mapped repsectively to I_5 and I_6. I_{11} and I_{12} are mapped respectively to I_9 and I_{10}. Finally, I_9 and I_{10} correspond escaping orbits. Thus we call I_9, I_{10}, I_{11} and I_{12} the immediate escape regions.

4.4 Periodic sequences and periodic orbits

In order to obtain periodic sequences, we make in Fig.5 a graph of transitory relations among I_i from the data in Table V. The necessary condition for a sequence to be periodic is to come back to some I_i starting from there. There are four shortest round trip paths in the figure: $I_1 \rightleftharpoons I_3$, $I_2 \rightleftharpoons I_4$, $I_5 \rightleftharpoons I_7$, and $I_6 \rightleftharpoons I_8$. However, the first two should be excluded. As we described in §4.3, these transitions correspond to secular movements in the respective areas, so no periodic sequences are expected to exist.

Let us consider transition $I_5 \rightleftharpoons I_7$. The form of a sequence in I_5 is $1.(2)^n 1 \ldots$, $n \geq 2$, whereas the form is $1.21(2)^2 \ldots$ in I_7. Then, the periodic sequence should contain a word $1(2)^n 12, n \geq 2$. Similarly, we get a word $12(1)^n 2$ from $I_6 \rightleftharpoons I_8$. We list first several ones in Table VI.

Table VI. Possible periodic symbol words.

5	6	7	8
12212	122212	1222212	12222212
12112	121112	1211112	12111112

Geometrically, periodic sequences can be obtained as crosspoints of curves or bands. Suppose that a word $1c_2 c_3 \ldots c_{n-1} 2$ is a unit of periodic sequence. Periodic sequence should be of the form $(2c_2 c_3 \ldots c_{n-1} 1)^\infty . (2c_2 c_3 \ldots c_{n-1} 1)^\infty$. Then sequence $1.(2c_2 c_3 \ldots c_{n-1} 1)^\infty$ is in one of I_i and sequence $1.(2\bar{c}_{n-1} \ldots \bar{c}_3 \bar{c}_2 1)^\infty$ is in another I_j. The corresponding periodic sequence is given as crosspoints of curves or bands $I(1.(2c_2 c_3 \ldots c_{n-1} 1)^\infty)$ and $I^t(1.(2\bar{c}_{n-1} \ldots \bar{c}_3 \bar{c}_2 1)^\infty)$ provided both sequences are allowable. Here, $I^t(1.(2\bar{c}_{n-1} \ldots \bar{c}_3 \bar{c}_2 1)^\infty)$ means the transformation of $I(1.(2\bar{c}_{n-1} \ldots \bar{c}_3 \bar{c}_2 1)^\infty)$ by $(\theta, R) \rightarrow (\pi - \theta, R)$. We show in Fig.5, the cases of periodic sequences $(22121)^\infty . (22121)^\infty$, $(222121)^\infty . (222121)^\infty$, and $(2222121)^\infty .$ $(2222121)^\infty$. Crosspoints are seen in small boxes. $(\theta, R) = (25.20951, 1.8645681)$ is the approximate position of $(22121)^\infty . (22121)^\infty$. In the figure, intersecting
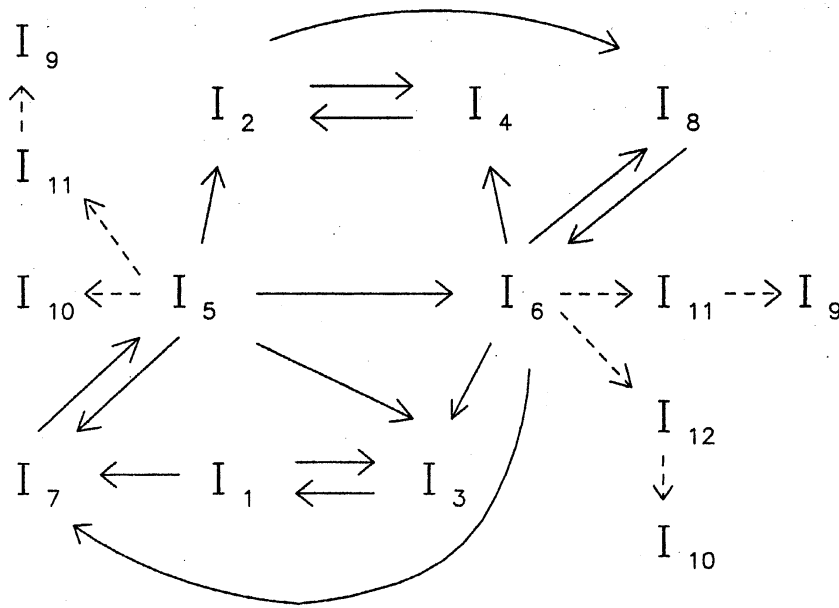
Figure 5: Graph for transitions among I_i.

curves are not continuous. This is due to the coarseness of the mesh of orbit integrations.

There are longer round trip paths. Let us list in Table VII all the possible round trip paths. Periodic words are obtained in a similar manner. These are also listed in Table VII. In the table, one sees $I_3 \rightleftharpoons I_1$ and $I_4 \rightleftharpoons I_2$ in the fourth, fifith, seventh and eighth paths. This means that the corresponding orbits repeat transitions between these regions as much times as the number of 21 in the sequences.

Table VII. Periodic paths and periodic words.

Path	Periodic word $(n, m \geq 2, k, k' > 0)$
$I_5 \rightleftharpoons I_7$	$1(2)^n 12$
$I_6 \rightleftharpoons I_8$	$12(1)^n 2$
$I_5 \rightarrow I_6 \rightarrow I_7 \rightarrow I_5$	$1(2)^n 12(1)^m 22$
$I_5 \rightarrow I_3 \rightleftharpoons I_1 \rightarrow I_7 \rightarrow I_5$	$1(2)^n 1(21)^{2k+1} 22$
$I_5 \rightarrow I_6 \rightarrow I_3 \rightleftharpoons I_1 \rightarrow I_7 \rightarrow I_5$	$1(2)^n 12(1)^m (21)^{2k} 22$
$I_5 \rightarrow I_2 \rightarrow I_8 \rightarrow I_6 \rightarrow I_7 \rightarrow I_5$	$1(2)^n 1(21)^{2k} 2(1)^m 22$
$I_5 \rightarrow I_2 \rightarrow I_8 \rightarrow I_6 \rightarrow I_3 \rightleftharpoons I_1 \rightarrow I_7 \rightarrow I_5$	$1(2)^n 1(21)^{2k} 2(1)^m (21)^{2k'} 22$
$I_6 \rightarrow I_4 \rightleftharpoons I_2 \rightarrow I_8 \rightarrow I_6$	$12(1)^n (21)^{2k} 2$

4.5 Property of the set of allowable Symbol Sequences

In this subsection, assuming the numerical results, it will be shown that allowable symbol sequences form a Cantor set. A *cylinder* is defined as a set of symbol sequences which has a fixed word in a give range of digits(see Robinson, 1995).

Assumption 4.2. Unallowable words are all given in Proposition 4.1.

Theorem 4.3. Under Assumption 4.2, the set Ω of allowable symbol sequences forms a Cantor set in Σ_2 and hence in Σ.

Proof. Cylinders are all open. Therefore, $\Omega = \Sigma_2 \backslash \{$all unallowable cylinders$\}$ is compact.

Take any allowable symbol sequence $s = (\ldots s_{-2}1.2s_1s_2, \ldots, s_n, \ldots)$. Let us suppose that there exists a sequence $1 < k_1 < k_2 < \ldots (k_i \to \infty$ as $i \to \infty)$ such that $s_{k_i} = 1$ and $s_{k_i+1} = 2$. Then s is not isolated. For, we have $\sigma^{k_i}s = (\ldots 1.2s_{k_i+2}s_{k_i+3} \ldots)$ and we know that there is an infinite number of allowable symbol sequences of this form. This implies that there are allowable symbol sequences in any neighborhood of s. s is not isoletaed in the case where there exists $N > 0$ such that $s_n = 1$ or $s_n = 2$ for $n > N$. For, we know the existence of symbol sequences of the form $.(2)^n121 \ldots$ or $.(1)^n212 \ldots$ for any $n \geq 2$.

In order to show that Ω is totally disconnected, it suffices to show that in any neighborhood of a sequence in Ω there is a sequence which does not belong to Ω. Using unallowable cylinders with their fixed words in arbitrarily high digits, we can construct a symbol sequence not belonging to Ω and arbitrarily close to a given allowable sequence. $\square$

As consequences, we have

Corollary 4.4. There is an uncountable number of non-escape orbits other than orbits in the Schubart region.

This is obvious because there is an uncountable number of symbol sequences other than $(21)^\infty.(21)^\infty$ and a symbol sequence corresponds to more than one orbits. Moreover, there may be an uncountable number of curves of initial conditions for non-escape orbits.

Corollary 4.5. The area of initial positions for a non-repeating symbol sequence is zero.

This is also obvious because the corresponding orbits appear infinite times in different positions of the surface of section.

5   Conclusions

We have demonstrated that symbolic dynamics is effective in the one-dimensional three-body problem. Main results are

(i) It has been found that there are unallowable sequences of binary collisions, the symplest ones being 2211 and 1122.

(ii) Periodic sequences are found and some of periodic orbits are positioned, the simplest one being $(22121)^\infty.(22121)^\infty$. The existence of oscillatory orbits with collisions is deduced.

(iii) Qualitative behavior of general orbits on the surface of section is understood to a certain extent by using symbol sequences and shift operator.

Acknowledgment

One of the authors(K.T.) expresses his thanks to Dr. Shigehiro Ushiki (Kyoto University) for useful suggestions on symbolic dynamics.

References

[1] Block, L.S. and Coppel, W.A., 1992, *Dynamics in One Dimension*, Lecture Notes in Mathematics Vol. 1513, Springer-Verlag.

[2] Bulirsch, R. and Stoer, J.:(1966), *Numerical Treatment of Differential Equations by Extrapolation Methods.* Num. Math., **8**, 1–13.

[3] Mikkola, S. and Hietarinta, J., 1989, *Celestial Mechanics and Dynamical Astronomy* **46**, 1-18.

[4] Mikkola, S. and Hietarinta, J., 1990, *Celestial Mechanics and Dynamical Astronomy* **47**, 321-331.

[5] Mikkola, S. and Hietarinta, J., 1991, *Celestial Mechanics and Dynamical Astronomy* **51**, 379-394.

[6] Robinson, C., 1995, *Dynamical Systems*, CRC Press, Boca Rayton, USA.

[7] Tanikawa, K. and Mikkola, S., 1999(Paper I), *Celestial Mechanics and Dynamical Astronomy*(submitted).

[8] Tanikawa, K. and Umehara, H., 1998, *Celestial Mechanics and Dynamical Astronomy* **70**, 167-180.

[9] Zare, K. and Chesley, S., 1998, *Chaos* **8**, 475-494.